# Modulation of Stem Cell Adhesion and Morphology via Facile Control over Surface Presentation of Cell Adhesion Molecules

*Haiqing Li[1], Jessica Frith[1], Justin J. Cooper-White[1,2,3,]**

[1] Tissue Engineering and Microfluidic Laboratory, Australian Institute for Bioengineering and Nanotechnology, The University of Queensland, Cnr Cooper and College Rd, Brisbane, 4072, Queensland, Australia.

[2] School of Chemical Engineering, The University of Queensland, College Rd, Brisbane, 4072, Queensland, Australia.

[3] CSIRO, Division of materials Science and Engineering, Clayton, 3169, Victoria, Australia.

ABSTRACT. To encourage cell adhesion on biomaterial surfaces in a more facile, safe, and low-cost fashion, we have demonstrated a non-covalent approach to spatially conjugate β-cyclodextrin (β-CD) modified peptide sequences onto self-assembled adamantane-terminated polystyrene-*b*-poly(ethylene oxide) (PS-PEO-Ada) films through inclusion complexing interactions between β-CDs and adamantane. By simply blending various ratios of unmodified PS-PEO with a newly synthesised PS-PEO-Ada, we produced PS polymer films that displayed

well-organized adamantine-decorated cylindrical PEO domains with varying average interdomain spacings ranging from 29 to 47 nm. The presence of the adamantane moiety at the terminal end of the PEO chain permitted rapid, and importantly, oriented attachment of β-CD functionalized peptides onto these surfaces. This one-step process not only converted these proven non-adherent PS-PEO surfaces into adherent surfaces, but also permitted precisely controlled presentation and surface distribution of the conjugated peptides. The utility of these surfaces as cell culture substrates was confirmed with human mesenchymal stem cells (hMSCs). We observed that with increasing PS-PEO-Ada content in the PEO cylindrical domains, these novel polymer films displayed improved cell attachment and spreading, with notable differences in hMSC morphology. We further confirmed that this novel PS-PEO-Ada surface provides a flexible platform for facile conjugation of mixtures of β-CDs functionalized with different peptides, specifically RGD and IKVAV peptides. The cell adhesion and spreading assays on these surfaces indicated that the morphologies of hMSCs can be easily manipulated, while no significant changes in cell attachment were observed. The 'lock-and-key' peptide conjugation technique presented in this work is applicable to any substrate that incorporates a moiety capable of forming inclusion complexes with α-, β- and γ-CDs, providing a facile and flexible method by which to construct peptide-conjugated biomaterial substrates for a multitude of applications in fields ranging from cell bioprocessing, regenerative medicine to cell-based assays.

## INTRODUCTION

The adhesion of cells to biomaterial surfaces is an important prerequisite for the successful integration of implants in vivo or the colonization of scaffolds intended for tissue engineering applications. To encourage cell adhesion, conventional man-made biomaterial surfaces typically

require pre-treatment, prior to them being further modified with either full-length extracellular matrix (ECM) proteins or conjugated with desired peptide sequences that can replicate sequences (in terms of number and type) available in full-length (ECM) proteins. Thus far, most of these pre-treatment protocols have involved a variety of chemical schemes, such as amination, esterification, click chemistry, and other multi-step reactions, depending on the functionalities presented on the biomaterial surfaces.[1-4] These reactions, however, tend to be carried out in the presence of toxic chemicals, under precisely controlled conditions (e.g. pH, temperature), and via tedious and time-consuming procedures, with limited options for the conjugation of multiple different peptide sequences. To address these drawbacks, we have developed a facile, one-step, water-based, low cost strategy to conjugate diverse peptides sequences onto biomaterial surfaces using cyclodextrins.

Cyclodextrins (CDs) are toroidally shaped polysaccharides with hydrophobic inner cavities. This unique molecular structure endows CDs with capacities to either partially or entirely accommodate suitably sized lipophilic guest moieties (e.g. aromatic compounds, ferrocene, cholesterol, and adamantane groups (in the case of β-CD)), forming a diverse set of host-guest inclusion complexes through facile hydrophobic and van der Waals interactions.[5-8] Taking advantage of these highly defined CD-guest interactions, CDs have been widely utilized in separation technologies, food processing, and pharmaceutical formulations.[9,10] Nevertheless, thus far there have been no reports of the utilization of these facile non-covalent interactions to conjugate peptide sequences onto biomaterial surfaces for cell adhesion.

Previously, it has been demonstrated by us that through the rapid self-assembly of asymmetric polystyrene-*b*-poly(ethylene oxide) (PS-PEO) on a hydrophobic substrate, it is possible to produce a thin film consisting of separated, vertically oriented cylinders constructed from a

number of PEO chains in a matrix of PS.[11,12] Moreover, the lateral spacing of these cylindrical PEO domain size can be effectively controlled by the molecular weight of PS-PEO, additional annealing treatment, and blending with PS homopolymer.[11-13] Particularly, our recent study revealed that the modification of PEO chain end with functional motif such as maleimide does not alter the nano-presentation of surface functionalities in terms of their distribution.[13] This finding opened a broad avenue for generating versatile PS-PEO substrates with well-controlled nano-presentation of surface functionalities. More recently, the control of nanoscale features of biomaterial substrates has been proven, by us and others, to be a powerful tool to regulate stem cell behaviours, such as adhesion, spreading, differentiation and apoptosis, by the surface nano-presentation of cell adhesive molecules.[14-18]

Herein, we present the synthesis and characterisation of adamantyl moiety functionalized PS-PEO (PS-PEO-Ada). We show that upon rapid self-assembly of PS-PEO-Ada, a polymer film bearing adamantyl motifs on the surfaces of cylindrical PEO nanodomains was generated. Taking advantage of the specific interaction between admantyl groups and β-CD, we confirm that β-CD modified peptide sequences (RGD and IKVAV) can be rapidly, non-covalently conjugated onto the PS-PEO-Ada films through a simple one-step incubation process (Scheme 1). Considering the unique surface nanostructures of the self-assembled PS-PEO-Ada films, we proposed that β-CD modified peptide conjugated PS-PEO-Ada films may be a viable culture platform for stem cells, and be capable of modulating their behaviors. In order to test this suggestion, and owing to their potential for tissue engineering and regenerative medicine applications, human mesenchymal stem cells (hMSCs) were cultured on the PS-PEO-Ada substrates.[19] The surface nano-presentation of these non-covalently conjugated peptide sequences were indeed shown to modulate the attachment and morphology of hMSCs in our current study,

proving the utility of this methodology for a multitude of cell culture and regenerative medicine applications.

Compared with more conventional methods of functionalizing biomaterial substrates with peptides to encourage cell adhesion and expansion, these novel surfaces have a number of advantages: 1) the peptide conjugation process was performed in neutral water, at room temperature, and in the absence of any additional chemicals, therefore it is a facile, safe and low cost protocol to bind and present cell adhesion molecules on biomaterial surfaces; 2) depending on the inter-domain spacing of PEO nanodomains, the surface distribution of the desired peptide sequence can be precisely tuned; 3) owing to the defined interaction between adamantyl groups and β-CD, multiple different CD modified peptide sequences can be conjugated onto the substrates, without having to consider the differences in reactivity and selectivity of the peptide sequences, as is the case in many conventional chemical reactions used in biomaterial functionalization. Analogously, as cyclodextrins, including α-, β- and γ-CD, form inclusion complexes with a diverse range of hydrophobic moieties (e.g. aromatic compounds, ferrocene, cholesterol, adamantane, poly(propylene oxide), etc.), it may be expected that any CD modified peptides can be conjugated onto a surface bearing the corresponding 'best fit' hydrophobic moieties for a given CD moiety by following the same protocol as developed here. Our protocol thus provides a very flexible methodology by which to construct biomaterial platforms with controllable nano-presentation of different peptide sequences.

## MATERIALS AND METHODS

### Materials

PS-PEO block copolymer, with a PS block molecular weight of 51 kDa and a PEO block of 11.5 kDa, was purchased from Polymer Source Pty. Ltd. (Montreal, PQ, Canada). β-CD was purchased from Sigma-Aldrich and purified by recrystallization in MilliQ water prior to use. CGRGDS and CGIKVAV peptides were supplied by Peptide 2.0 Inc. (Chantilly, VA, USA) and used as received. Sulfosuccinimidyl 4-[*N*-maleimidomethyl]cyclohexane-1-carboxylate (Sulfo-SMCC) was purchased from ProteoChem. 1-Adamantyl isocyanate, Di-n-butyltin dilaurate (DBTL), anhydrous toluene and N,N-dimethylformamide (DMF), and all chemicals for synthesis of amine mono-substituted CD were purchased from Sigma-Aldrich and used as supplied. All materials for hMSCs culture, staining and imaging were purchased from Sigma unless otherwise stated.

**Synthesis of PS-PEO-Ada**

Dry PS-PEO (625 mg) and 1-adamantyl isocyanate (90 mg) were dissolved in 10 mL of anhydrous DMF with vigorous stirring in nitrogen atmosphere, followed by the addition of DBTL (2.2 mg). The reaction temperature was elevated to 80 $^{o}$C and left to react for 24 h. The reaction mixture was dialyzed against chloroform at room temperature for 3 days. After removing solvent by rotor-evaporation, a white PS-PEO-Ada polymer solid was collected and further dried under vacuum overnight.

**Synthesis of β-CD modified peptides**

Amine mono-substituted β-CD (CD-$NH_2$) was firstly synthesized as described previously.[20] To synthesize β-CD modified peptides, CD-$NH_2$ (3.6 mg, 3.2 μmol) and sulfo-SMCC (1.1 mg, 3.2 μmol) was dissolved in 2.0 mL of phosphate buffered saline (PBS) aqueous solution with gentle stirring. After the reaction proceeded for 1 h, 6.4 μmol of peptide (CGRGDS and CGIKVAV ) was added into the reaction mixture, followed by another 4 h of reaction. β-CD modified peptide

solutions (CD-RGD and CD-IKVAV) were obtained and further diluted with 10 mL of PBS solution.

**Preparation of peptide-conjugated polymer surfaces**

Glass slides (13 mm in diameter) were exposed to UV/ozone for 20 min to remove any organics. The slides were then rendered hydrophobic by boiling in benzyl alcohol for 4 h, and further rinsed thoroughly in isopropanol and dried under a stream of nitrogen. Polymer films were generated by spin casting polymer solutions in toluene (2% wt/vol) onto the treated glass slides at 2000 rpm. The polymer coated glass slides were then transferred to a 24-well plate with 0.5 mL of diluted β-CD modified peptide solution (0.32 mM) in each well and left to incubate for 8 h at room temperature. Thereafter, the surfaces were thoroughly rinsed in MilliQ water to remove any un-reacted chemicals and excess amounts of peptides.

**Material characterization**

*$^{1}$H NMR and X-ray photoelectron spectroscopy (XPS) spectra*: $^{1}$H NMR spectra of the polymer samples were acquired at 298 K in deutorochloroform ($CDCl_3$) on a Bruker Avance 750 spectrometer. XPS analysis was performed using an ESCALAB 250 from Thermo VG Scientific. Monochromatic Al Kalpha X-rays were used (15 kV, 150 W, ~500 μm spot diameter). The transmission function of the analyzer was calibrated using a standard copper sample. Spectra were measured using a pass energy of 80 eV for survey spectra.

*Quartz crystal microbalance with dissipation monitoring (QCM-D)*: A Q-Sense QCM-D E4 was used to in-situ monitor the conjugation of β-CD modified peptides onto PS-PEO-Ada surfaces. Briefly, QCM crystal was pre-coated with a PS-PEO-Ada layer on a gold substrate following the procedures described above. The crystals were then thoroughly rinsed in MilliQ water and dried under a stream of nitrogen. Thereafter, a PS-PEO-Ada film was mounted onto the treated crystals

by spin coating PS-PEO-Ada solution in toluene (20% w/v) at 2000 rpm. After a polymer coated crystal and a bare treated crystal were assembled into the QCM-D instrument, PBS solution was continuously injected into the QCM chamber at a rate of 50 μL/min, and the system was equilibrated for 30 min. After confirming a stable baseline, the PBS solution was then replaced with a CD modified CGRGD solution in PBS. Once the frequency and dissipation curves again reached their new baseline, the injection solution was replaced with a fresh PBS solution to rinse away any freely absorbed molecules. The QCM-D data was analyzed using QTools software.

*Water contact angle*: The water contact angles of the substrates were determined by a sessile drop method at 25 $^{o}$C using a contact angle goniometer (CAM 100, KSV Instruments Ltd.). A 5 μL droplet of water was placed on the substrates. All samples were prepared as triplicates and the results shown are the mean value with a single standard deviation.

*Atomic force microscopy (AFM)*: Imaging of the self-organized polymer films on glass slides was carried out on a Multimode Nanoscope-IIIa Scanning Probe Microscope (Digital Instrument Co., Ltd. U.S.A.) equipped with a NT-MDT silicon cantilever (NSCII, radius < 10nm, resonance frequency = 300 kHz, nominal spring constant = 42 N/m, vertical resolution < 0.03 nm, lateral resolution < 2 nm) by using the AC mode at room temperature. The AFM is mounted on an anti-vibrational table (Herzan) and operated within an acoustic isolation enclosure (TMC, USA).

**hMSC culture, staining and imaging**

*Cell culture:* Human bone-marrow MSC (hMSC, supplied by Dr Gary Brook at the Mater Medical Research Institute, Brisbane, Australia) were cultured in low-glucose DMEM supplemented with 100 U/mL penicillin, 100 ug/mL streptomycin (DMEM/ps) and 10% batch-tested foetal bovine serum (FBS) at 37 $^{o}$C in 5% $CO_2$ in an atmosphere with 95% humidity. Upon reaching 70% confluence, hMSCs were passaged and reseeded at an approximate density

of 2000 cells/cm$^2$. Prior to seeding the cells onto PS-PEO-Ada–peptide surfaces in serum-free media (DMEM/ps and 1% ITS+; Sigma), MSCs were detached with TrypLE Select (Invitrogen), resuspended in 1% bovine serum albumin (BSA) in PBS then washed thoroughly.

*Cell attachment assays:* Prior to use in cell culture experiments, PS-PEO-Ada–peptide surfaces were sterilized by immersing them in ethanol sol (75%) for 10 min, followed by thoroughly rinsing with PBS. hMSCs were seeded onto PS-PEO-Ada–peptide surfaces at a density of 3000 cells/cm$^2$ in serum-free media and allowed to attach for 2 hours. Attachment levels were determined by Crystal Violet assay. Briefly, surfaces were washed twice in PBS to remove unattached or weakly attached cells, and the remaining cells then fixed in 4% paraformaldehyde (Sigma-Aldrich, Sydney, Australia) for 20 minutes and stained with 0.1% (w/v) Crystal Violet (Sigma-Aldrich) in 200 mM 2-(Nmorpholine) ethanesulfonic acid (Sigma-Aldrich), pH 6.0 for 10 minutes. Cells were washed five times in MilliQ water to remove excess Crystal Violet before the addition of 100 ml of 10% glacial acetic acid. Absorbance was read at 590 nm using a Spectramax M5 Fluorometer (Molecular Devices).

*Analysis of cell morphology*: hMSCs were cultured on the peptide conjugated PS-PEO-Ada surfaces at a density of 3,000 cells/cm$^2$ in serum-free media for a period of 24 hours, washed in PBS and fixed for 10 minutes in 4% paraformaldehyde. The cells were then permeabilized in 0.1% Triton X-100 in PBS for 5 minutes, and stained with Hoechst and FITC-phalloidin. Samples were rinsed thoroughly in PBS and mounted onto glass slides in Vectashield containing DAPI (Vector Laboratories). The cells were imaged using an Olympus BX61 fluorescent microscope. The resulting images were analysed using ImageJ 1.42 software (NIH, Bethesda, MD).

## RESULTS AND DISCUSSION

**Polymer surfaces with tunable surface architectures.** PS-PEO-Ada was synthesized by reacting the hydroxyl pendant group on the PEO block of the PS-PEO polymer and adamantyl isocyanate in the presence of DBTL. The synthesis of PS-PEO-Ada was confirmed by $^{1}$H NMR analysis (Figure 1a). Compared with unmodified PS-PEO, PS-PEO-Ada demonstrated new shifts situated at 1.69, 2.01 and 2.09 ppm, corresponding to the $H^{1}$ chemical shifts of adamantyl groups on the polymer chain end.

*Figure 1. here*

Upon rapid self-assembly, PS-PEO can self-organize into a thin film with well-defined cylindrical PEO domains uniformly distributed into PS matrix (Figure 2a). As determined by AFM observation, the average inter-domain spacing the PEO domains was 29.0 nm. The PEO domain diameter was 16.4±1.4 nm, respectively (Figure 2a and 2e). To highlight the use of the polymer films with well controlled surface nano-presentation of peptide sequences, the polymer surfaces bearing different densities of adamantyl groups in PEO domains, and thus controlled numbers of non-covalently conjugated β-CD modified peptide sequences in each nanodomain, were generated by co-self-assembly of PS-PEO with different amounts of PS-PEO-Ada. Interestingly, when 25 wt% of PS-PEO-Ada was mixed with PS-PEO, a polymer film with well-organized cylindrical PEO domains of dia. 16.8±1.5 nm was achieved (Figure 2b). Following a similar blending technique, further increases in the amount of PS-PEO-Ada up to 50 wt% and 75 wt% resulted in the formation of polymer films with significantly increased average inter domain spacings, being 39 and 47 nm, respectively, but only slight increases in domain diameters (17.2±2.0 and 18.9±2.2 nm). Moreover, all the resultant blended polymer films presented well-

defined cylindrical PEO domains (Figure 2c-2e). Further AFM analysis confirmed that the self-assembly of pure (100%) PS-PEO-Ada resulted in a thin film with irregular surface nanostructures, differing substantially from that of the PS-PEO and the PS-PEO-Ada blended systems (Figure 2f). However, if a line plot is made of this surface, whilst the surface lacks clearly defined separation between domains in some regions, the majority of structure are separated by an inter-domain spacing of between 35 to 105 nm, and the nanodomains have cross sections ranging from 21 to 55 nm.

*Figure 2 here*

The β-CD modified RGD and IKVAV were synthesized by linking amine-monosubstituted β-CD and cysteine terminated RGD and IKVAV using sulfo-SMCC as a coupling agent. Taking advantage of the formation of an inclusion complex between adamantane with β-CD, these β-CD modified peptides can be easily conjugated onto PS-PEO-Ada surfaces through facile non-covalent interactions. To evidence this assumption, after the self-assembled PS-PEO-Ada film was conjugated with β-CD modified peptide sequences, and then thoroughly rinsed in MilliQ water to remove any un-reacted products, the resultant surface was subjected to XPS analysis (Figure 1b). In comparison to the bare PS-PEO-Ada films, both CD-RGD and CD-IKVAV conjugated PS-PEO-Ada surfaces exhibited a sharp N1s peak at 398 eV, proving the successful conjugation of peptide sequences on the polymer surfaces. However, no feature N1s peak was observed on PS-PEO surface that was incubated with CD-RGD for 18 h followed by a thorough rinse with MilliQ water. This fact proved that the conjugation of CD modified peptides on PS-PEO-Ada surface is through the selective interactions between CD and adamantane group rather than nonspecific physisorption interactions.

To further characterise this peptide conjugation process, the time course of Δf upon exposure of the polymer coated QCM crystal to a CD-RGD solution in PBS (0.3 mM) was recorded at 25 $^{o}$C (Figure 3a). In the case of 75% PS-PEO-Ada coated QCM crystal, after injection of the CD-RGD solution at 50 uL/min, there was a gradual decrease in the resonant frequency, accompanied by a slow shift in the dissipation, evidencing continuous adsorption of the CD-peptide onto the PS-PEO-Ada surfaces. After 340 min, Δf reached equilibrium, indicating a saturated surface of immobilized CD-RGD. Thereafter, rinsing the peptide immobilized surfaces with PBS had little effect on Δf, which suggests an irreversibly bound CD-RGD. According to the equilibrium values of Δf obtained after rinsing with PBS, the surface binding CD-RGD amount was calculated as 19.5 ng/cm$^2$ through a Sauerbrey relation.[21] In addition, the QCM data showed that the achievement of saturation of binding of CD-RGD on the 75% PS-PEO-Ada surface required a significant amount of time (~ 340 minutes). This is due to the fact that on this particular polymer surface, the adamantane motifs decorate not only to top surface or outer perimeter of the PEO nanodomains, but also all of the inner walls of each cylindrical PEO nanodomains that penetrate into the depth of the film. As discussed in more detail below, this surface thus has a significant binding capacity for any conjugate, supporting the timeframe of surface saturation. Furthermore, the actual rate of binding of modified CDs to the surface is relatively constant, as shown by the consistency in the d(Δf )/dt during the conjugation event, corresponding to ~55 pg/cm$^2$/min, a reasonable rate considering that this process will be diffusion-dominated.

The outer perimeter of each PEO cylinder of diameter 19 nm is composed of approximately 27 PEO chains (based on a hydrodynamic radius of each PEO chain (11000 g/mol) of ~ 2.2 nm (calculated according to the method described in [22])). The functionalised β-CD-RGD is

estimated to be of a similar size to the PEO (β-CD alone is 1.66 nm), meaning that at maximum packing on the outer rim of one cylinder composed of 75% PS-PEO-Ada, we may obtain ~27 conjugated CD-RGD molecules. Further, each PEO cylinder is of a height of ~ 40 nm (determined from film thickness measurements using ellipsometry and X-ray reflectometry),[23] meaning that in addition to the top most surface-exposed layer of the PEO chains within these cylinders, there are approximately 18 additional layers of PEO chains protruding into the cylinder over its length. Therefore, in each cylinder composed of 75% PS-PEO-Ada, there are a total of ~364 PEO-Ada binding sites for CD-RGD. At an inter-cylinder spacing of 47 nm, and a total molecular weight of ~ 1964 g/mol for the CD-RGD molecule, we would thus estimate that at 100% conjugation, we should measure a mass of 59.2 ng/cm$^2$ on our 75% PS-PEO-Ada surface. However, due to steric hindrance and chain effects, we would expect to achieve a lower level of conjugation than 100%. Our measured mass of 19.5 ng/cm$^2$ actually equates to a conjugation level of CD-RGD on the 75 % PS-PEO-Ada surfaces of 33%, or ~ 7 CD-RGD molecules (on average) conjugated on the top most surface-exposed layer of each PEO cylinder, that would be available for cell binding. Further QCM tests indicated that 25% , 50%, and 100% PS-PEO-Ada substrates exhibited the similar CD-RGD binding kinetics to that of 75% PS-PEO-Ada substrate. The measured mass on 25%, 50%, and 100% PS-PEO-Ada substrates is 8.8, 14.9, and 25.2 ng/cm$^2$, respectively. Thus the corresponding conjugation levels of the CD-RGD on those surfaces are 44%, 38%, and 32%, respectively. We thus estimate that there would be ~ 4 CD-RGDs per 17.2 nm (dia.) cylinder on the 50% PS-PEO-Ada surface, and ~ 2 CD-RGDs per 16.8 nm (dia.) cylinder on the 25% PS-PEO-Ada surface. In contrast, bare PS-PEO surface showed little CD-RGD binding, further evidencing that bind of CD-RGD on the polymer

surfaces is through the specific CD-adamantane interactions rather than the non-specific physical absorptions.

From the water contact angle measurement results shown in Figure 3b, the water contact angle of (75%) PSPEO-Ada surface was significantly decreased from 83.9±1.2 $^{o}$ to 32.9±2.5 $^{o}$ after CD-RGD conjugation (Figure 3b). This significant change in surface wettability further confirmed the conjugation of our CD-RGD to the polymer surfaces.

*Figure 3 here*

**Nanoscale spatial distributions of RGD peptide regulated hMSC adhesion**. Encouraged by the recent reports of surface-regulated stem cell behaviours, we investigated the effect of the CD-RGD modified PS-PEO-Ada surface on hMSC attachment and morphology. After 2 h of culture on these surfaces, hMSC attachment was quantified by crystal violet staining. As shown in Figure 4, rather low cell adhesion was evident on PS-PEO alone, on PS-PEO-Ada alone, or on PS-PEO surfaces that had been incubated with CD-RGD (prior to the addition of cells). In contrast, the CD-RGD conjugated polymer surface containing 25 wt% of PS-PEO-Ada exhibited significantly enhanced hMSC attachment. This result suggests that hMSC adhesion is being mediated specifically by the surface conjugated CD-RGD, rather than by the physiosorption of the CD-RGD onto the PS-PEO polymer surfaces. The CD-RGD conjugated surfaces with 50 wt% of PS-PEO-Ada content demonstrated a further increase in hMSC adhesion, to a similar level to that achieved on tissue culture plastic (TCP, positive control). However, no further improvement in cell adhesion was observed on the polymer surfaces with further increased PS-PEO-Ada content (up to 75 wt%), nor at 100 wt% (pure PS-PEO-Ada surfaces). This trend in hMSC attachment being dependent on the PS-PEO-Ada content in the substrate is related to the

density of surface binding RGD motifs. At 50 wt% of PS-PEO-Ada component, the number of adamantane moieties presented on the self-assembled polymer surfaces obviously reached a level at which the number of surface-conjugated CD-RGDs was sufficient enough for maximal cell adhesion and thus any further increase in the number of binding sites for CD-RGD through additional adamantane moieties within the PEO cylinders did not lead to a continuous improvement on the cell adhesion. This is likely due to the increasing levels of ligand redundancy (in terms of available integrin-ligand binding sites) within each of the PEO cylinders as the amount of PS-PEO-Ada in the substrate increases.

*Figure 4 here*

After hMSCs were seeded on the surfaces with different contents of PS-PEO-Ada (0-100 wt%) for 24 h, the morphologies of the resulting spread cells were investigated using Confocal Fluorescence Microscopy. The very few cells poorly adhered to the PS-PEO surfaces exhibited non-polarized and rounded morphologies and had a poorly organized actin cytoskeleton with no stress fibres (Figure 5a). No obvious changes in cell morphology were observed post the incubation of this surface with solubilised CD-RGD, suggesting, as expected, that no RGD was immobilized on PS-PEO surface (Figure 5b). However, with increased content of PS-PEO-Ada in the PS-PEO polymer films, and post incubation of these surfaces with solubilised CD-RGD, an increase in the proportion of hMSCs with spread morphologies was observed (Figure 5c-e). In particular, the cells on CD-RGD conjugated 100% PS-PEO-Ada surface demonstrated highly polarized, well spread morphologies, with a well-organised actin cytoskeleton and multiple stress fibres (Figure 5f). In contrast, the cells on the 100% PS-PEO-Ada alone surface (without the CD-RGD incubation step) displayed rounded shapes and significantly decreased spreading and had a poorly organized actin cytoskeleton (Figure 5g). Using ImageJ image analysis, the average cell

spread areas of the attached hMSCs was calculated and plotted as function of the content of PS-PEO-Ada in the PS-PEO polymer substrates (Figure 5h). As expected, hMSCs on the non-RGD-conjugated PS-PEO-Ada exhibited a round morphology with a slightly increased spread area (1400 $\mu m^2$) compared to the bare PS-PEO surface (980 $\mu m^2$), but with a much lower spread area than that of CD-RGD conjugated 100% PS-PEO-Ada surfaces (3530 $\mu m^2$). With an increasing content of PS-PEO-Ada in the substrates, and thus increasing number density of RGD-modified CD *within* each nanodomain (of near equivalent diameters (~17 – 19 nm)), the average spread area of hMSCs increased from 1488 $\mu m^2$ on the 25% CD-RGD conjugated PS-PEO-Ada surface (interdomain spacing of 29nm) to 2718 $\mu m^2$ on 75% CD-RGD conjugated PS-PEO-Ada surface (interdomain spacing of 47 nm). Given our previous insights into the effects of nano-scale presentation of covalently-bound adhesion motifs on hMSC differentiation,[16] these significant changes in morphology and spread area of hMSCs suggests that the differentiation of hMSCs may be also manipulated on these non-covalently conjugated RGD substrates, emphasising the potential of these surfaces for stem cell selection and fate control.

However, intriguingly, the increasing inter-domain spacings of 30 to 47 nm apparent with increasing amounts of PS-PEO-Ada from 25 to 75%, we may have expected to see reductions in mesenchymal stem cell spread area of approximately 24%, as we have previously reported when increasing the lateral spacing of similarly sized PEO nanodomains (~ 12 nm) presenting covalently bound RGD motifs.[16] Similar results were also achieved in Spatz's group with MC3T3 osteoblasts, where they revealed that the increase of inter-spacing of cyclic RGDfK peptides patches caused a significant decrease of cell spread area.[17] Even though 100% PS-PEO-Ada surface has no well-defined nanopatterns, the existence of 35~105 nm inner-domain spacings between the separated domains also is expected to lead to a significant decrease in

hMSC cell area. However, we in fact observed just the opposite in this current work, with a significant *increase* in spread area.

Due to the inherent tunability of these PS-PEO/PS-PEO-Ada surfaces, in terms of the number of adhesion motifs able to be conjugated within one nanodomain, we are now able to provide new insight into the manner by which adhesion motifs displayed to hMSCs affect their adhesion and morphology. This data shows that increasing the number of the cell adhesive ligands *within* the nano-sized domains can affect greater control over cell adhesion and cell spread area than any increases in inter-domain spacing, at least over the range of ~30 – 50 nm. However, the limitation in size of the nanodomains under all conditions (in the range of that of a single integrin [24]) means that this effect cannot be attributed to an enhanced ability of the substrates containing PS-PEO-Ada to support integrin clustering (which is a prerequisite for focal adhesion formation and subsequent stress fibre formation) due simply to spatial orientation, in the manner described by Maheshwari et al [25] who used star-PEGs to present differing cluster sizes of RGD peptides. This outcome is instead believed to be due to *increased ligand redundancy*. As the number of CD-RGDs within a nanodomain increases, these substrates offer increased ligand redundancy for integrin-ligand binding. Rossier *et al*. have recently shown that within focal adhesions, whilst our previous understanding may have suggested that integrins are *stably* adherent, they in fact undergo repeated anchoring cycles, constantly switching between active and inactive states.[26] The increased ligand number in each nanodomain thus creates a higher probability of longer time *localized* integrin-ligand binding events, which will result in increased focal adhesion stability and maturation. This will result in greater force transmission, maturation of the actin cytoskeleton and increased spreading.

**Effects of peptide sequence type on the hMSC adhesion**. As these CD modified peptides enable conjugation to our adamantane-containing surfaces through non-covalent inclusion complex interactions, it is now clearly possible to quantitatively conjugate different types of (and ratios thereof) CD modified peptides onto those polymer surfaces. We thus next explored the immobilization of different blends of two different CD-conjugated peptides onto our 100% PS-PEO-Ada surface following the same conjugation protocol. As well as the commonly used RGD cell attachment sequence derived from Fibronectin, we also tested a Laminin-derived motif, IKVAV. As is expected, 100% PS-PEO-Ada surface exhibited the similar CD-IKVAV conjugation kinetics to that of CD-RGD (Figure 6). Determined by QCM, the measured mass and the calculated conjugation level of CD-IKVAV on 100% PS-PEO-Ada surface are 27.1 ng/cm$^2$ and 34% , respectively. This fact evidenced that the investigated surfaces had the similar CD-IKVAV conjugation level to that of CD-RGD (32%).

*Figure 6 here*

After 2 h of culture with hMSCs, all the surfaces conjugated with different ratios of RGD and IKVAV exhibited similar levels of cell adhesion to that of the TCP substrate, as determined by crystal violet staining (Figure 7). As described earlier, after 24 h of cell culture, hMSCs cultured on CD-RGD conjugated PS-PEO-Ada surfaces showed well spread morphologies and well-organised actin with multiple stress fibres (Figure 4h). However, when we increased the amount of CD-IKVAV within the blends of CD-peptides on the PS-PEO-Ada surfaces, in the range from 25 mol% to 75 mol %, an increase in the number of hMSCs displaying a round morphology was observed (Figure 8a-8c). The average cell spread area also decreased and the cytoskeletal architecture changed, with cells showing a switch from highly aligned stress-fibres spanning the length of the cell, to smaller, less well-organised fibres. When the hMSCs were cultured on a

100% CD-IKVAV conjugated PS-PEO-Ada surface, the majority of cells displayed rounded shapes, with significantly decreased average cell spread area and poorly organized actin that was predominantly localized to the cell periphery (Figure 8d). Figure 8e shows the decreasing trend of average cell spread area depending on the amount of CD-RGD peptide in the blend. This ability to systematically vary morphologies and cell spread areas of stem cells by simply changing the ratios of CDs (modified with different adhesion peptides) added to the substrate prior to cell culture represents a truly enabling technology platform.

*Figure 7 and Figure 8 here*

## CONCLUSIONS

In this paper, we have demonstrated a facile approach to conjugate β-CD modified peptide sequences (CD-RGD and CD-IKVAV) onto self-assembled PS-PEO-Ada films through non-covalent interactions between β-CDs and adamantane motifs. Upon simply blending different contents of PS-PEO-Ada with PS-PEO, the self-organized polymer films exhibited controllable differences in average lateral spacings of PEO domains, and thus permitted precisely controlled surface nano-presentation of peptide sequences. Depending on the density of surface bound CD-RGD, hMSCs showed increased adhesion and variations in morphology, ranging from rounded to highly spread, with associated changes in cytoskeletal organization from a disorganized actin cytoskeleton to well-defined and highly aligned stress fibres. By simply mixing different amounts of CD-RGD and CD-IKVAV, PS-PEO-Ada films with tuned surface presentation of different peptides were also generated. The cell adhesion assays on these surfaces revealed that the morphologies of hMSCs can be effectively manipulated, from rounded cells with lower spread areas on IKVAV conjugated substrates, to well spread cells with significantly increased

spread area on RGD conjugated surface, yet the initial adhesion was similar in terms of cell number. Such differences in hMSC spreading and cytoskeletal organisation have been shown to influence the differentiation of hMSC populations and therefore suggest future potential for the surfaces described herein to help direct the fate of hMSCs in tissue engineering applications. It is worth noting that the facile 'lock-and-key' peptide conjugation technique presented in current work is also applicable to fabricate a wide range of peptide-conjugated biomaterials through the unique inclusion complexing interactions between cyclodextrins and specific moieties.

FIGURES.

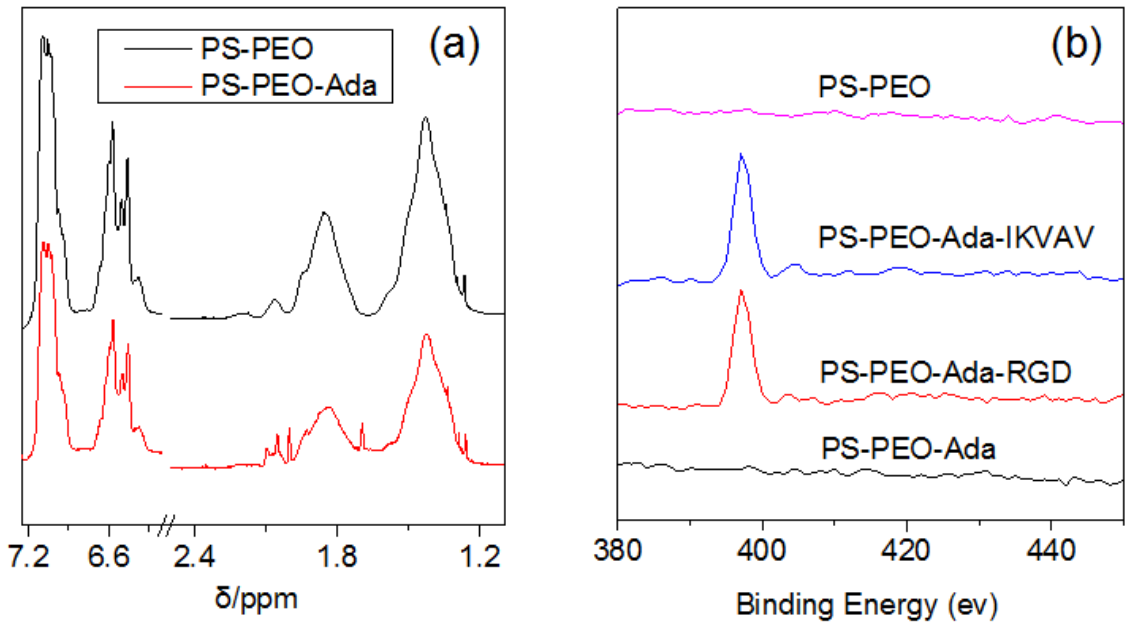


**Figure 1.** $^{1}$H NMR spectra of PS-PEO and PS-PEO-Ada (a), and N1s XPS spectra of PS-PEO, and PS-PEO-Ada films before (PS-PEO-Ada) and after conjugation with CD-RGD (PS-PEO-Ada-RGD) and CD-IKVAV (PS-PEO-Ada-IKVAV) moieties (b).

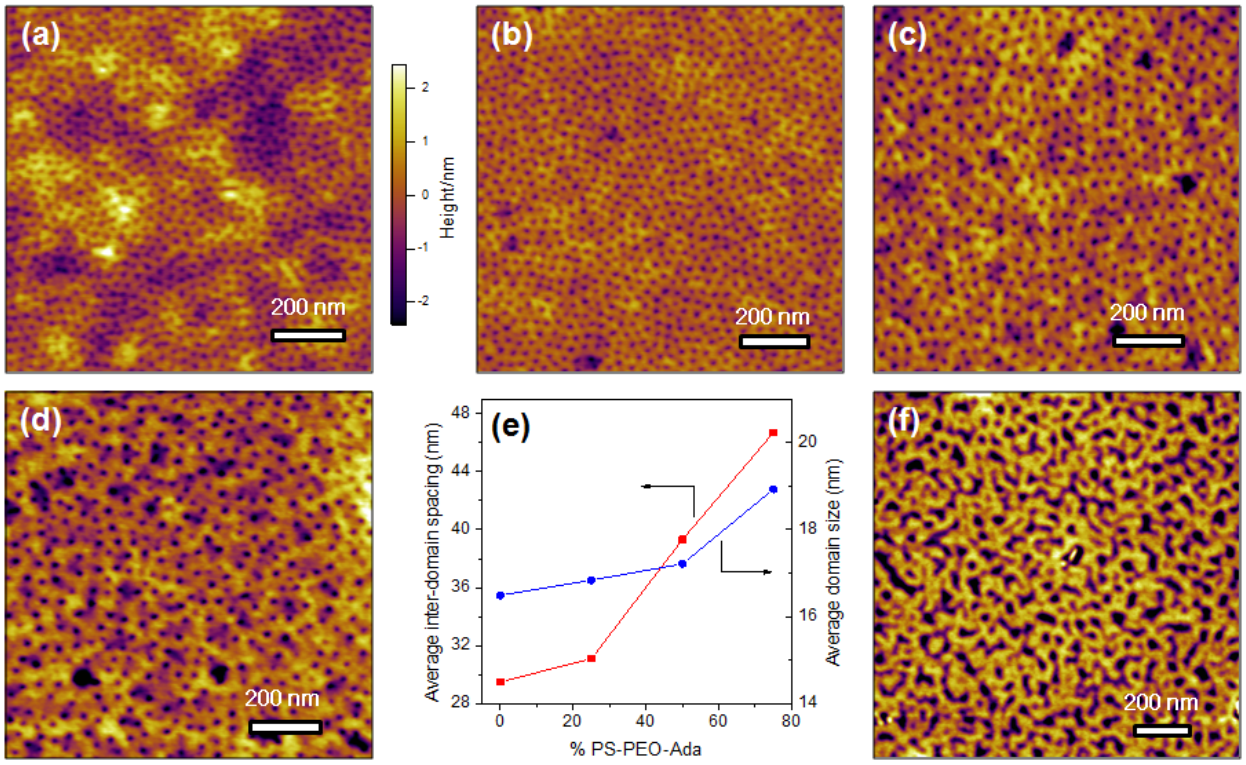


**Figure 2.** AFM height images of polymer substrates obtained from self-assembly of (100%) PS-PEO (a), and co-self-assembly of PS-PEO with 25% (b), 50% (c), 75% (d) of PS-PEO-Ada; the calculated average PEO domain size and inter-domain spacing of the resultant polymer films (e); AFM image of self-assembled (100%) PS-PEO-Ada (f).

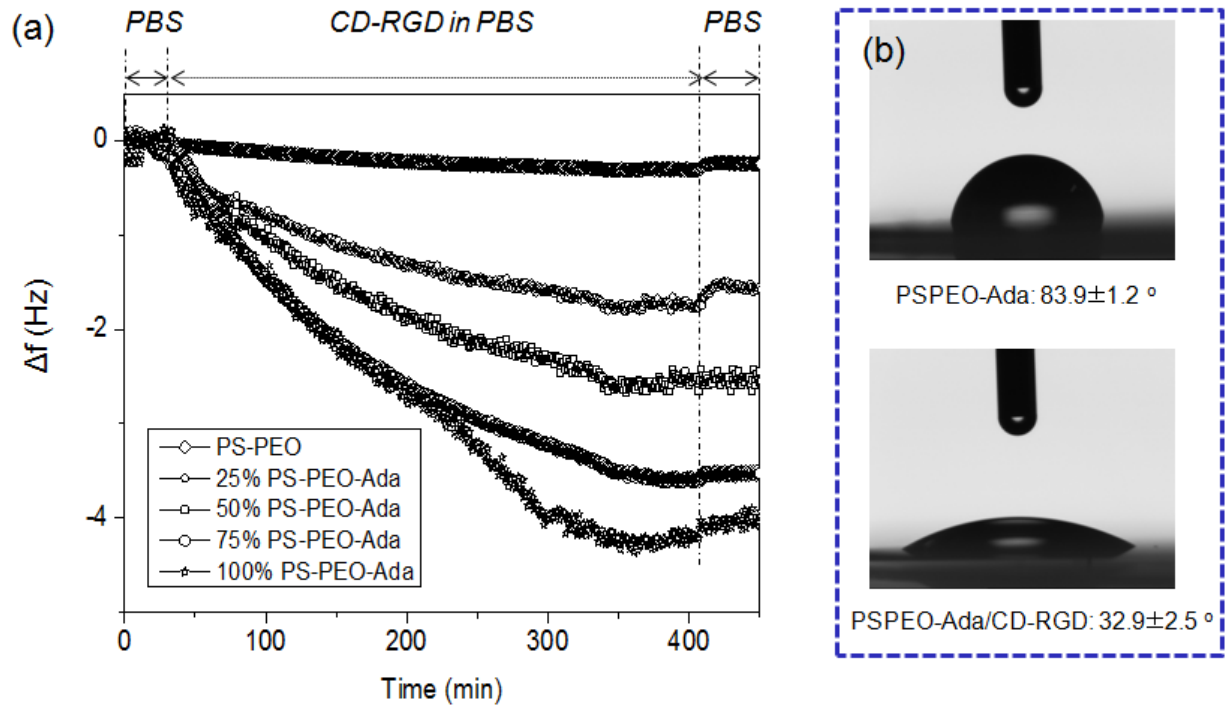


**Figure 3.** QCM-D response curves, in terms of changes in frequency, during the non-covalent conjugation of CD-RGD to the self-assembled PS-PEO, PS-PEO-Ada, and their blend surfaces (a); water contact angle of 75% PS-PEO-Ada surface before and after being conjugated with CD-RGD (b).

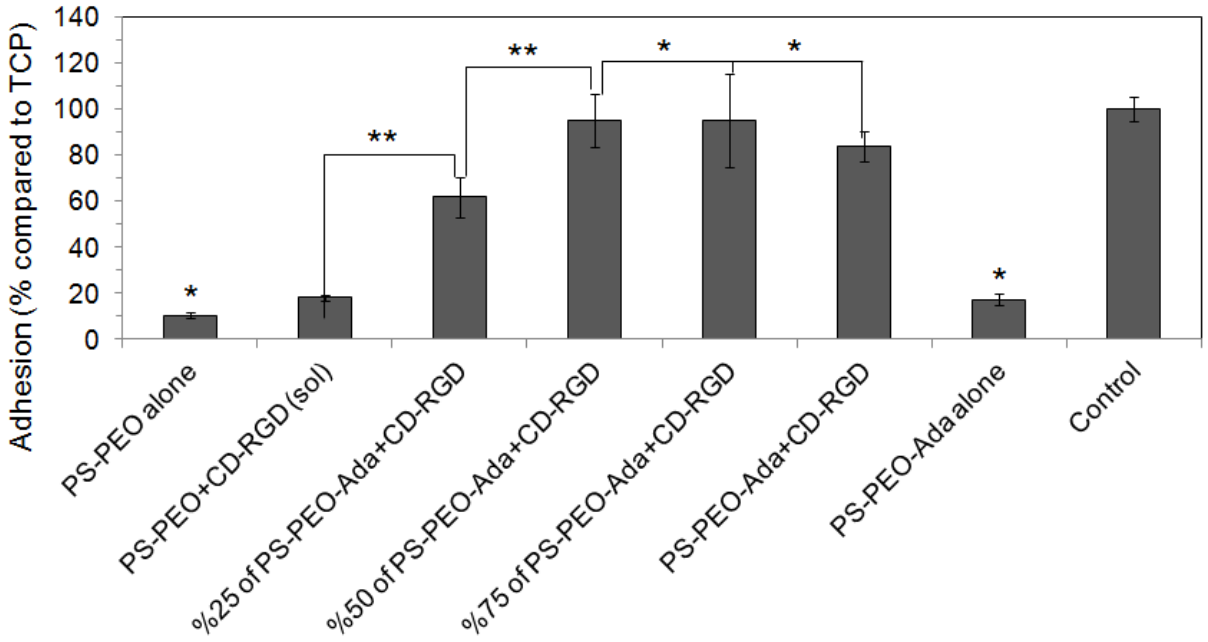


**Figure 4.** Adhesion of hMSCs to β-CD-RGD non-covalently conjugated polymer substrates obtained by the co-self-assembly of PS-PEO with different content of PS-PEO-Ada. Control is TCP (without β-CD-RGD). Error bars represent mean ± SD for n = 4, (*) $p < 0.05$, (**) $p < 0.01$. All the cells were cultured on the substrates at a density of 3,000 cells/cm$^2$ in serum-free media for a period of 2 hours.

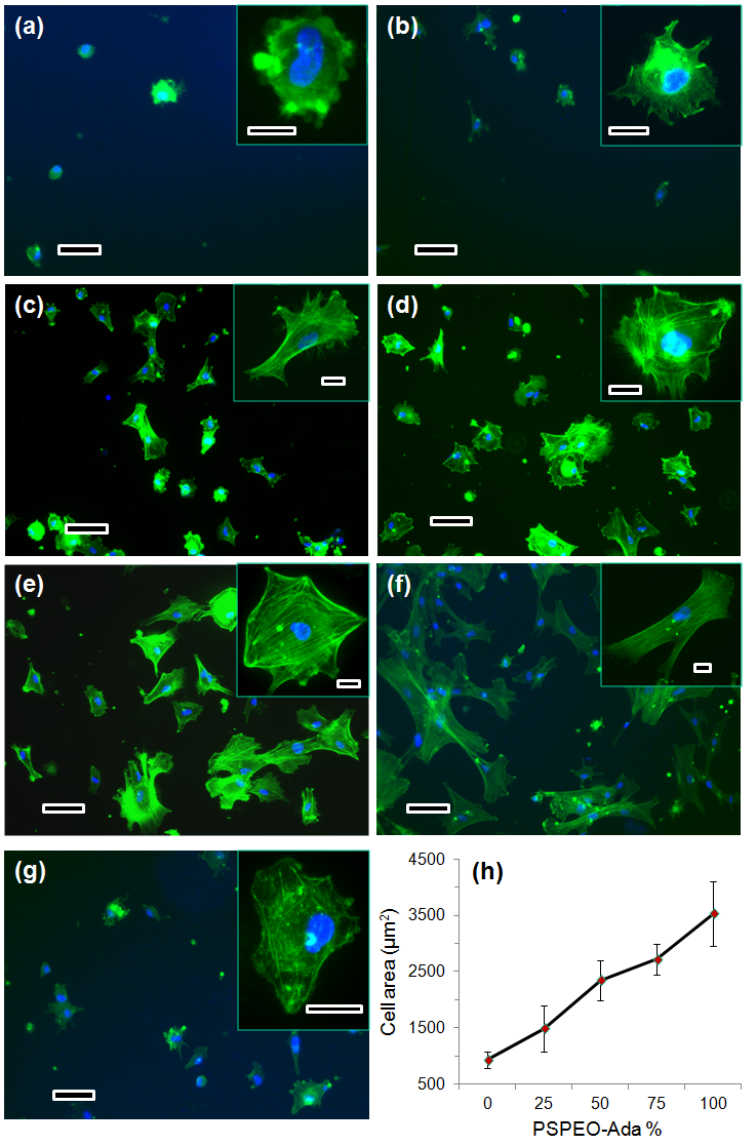


**Figure 5**. Fluorescent microscopy images of hMSCs on different polymer surfaces: PS-PEO alone (a); PS-PEO incubated in the presence of CD-RGD (b); CD-RGD conjugated polymer surfaces constructed by co-self-assembly of PS-PEO with 25 wt% (c), 50 wt% (d), and 75 wt% (e) of PS-PEO-Ada; 100% PS-PEO-Ada surface with (f) and without (g) CD-RGD conjugation; average cell area as function of surface content of PS-PEO-Ada (h). The scale bars in (a)-(g) are 100 μm. Inset scales bars 20 μm. All the cells were cultured on the substrates at a density of 3,000 cells/cm$^2$ in serum-free media for a period of 24 hours.

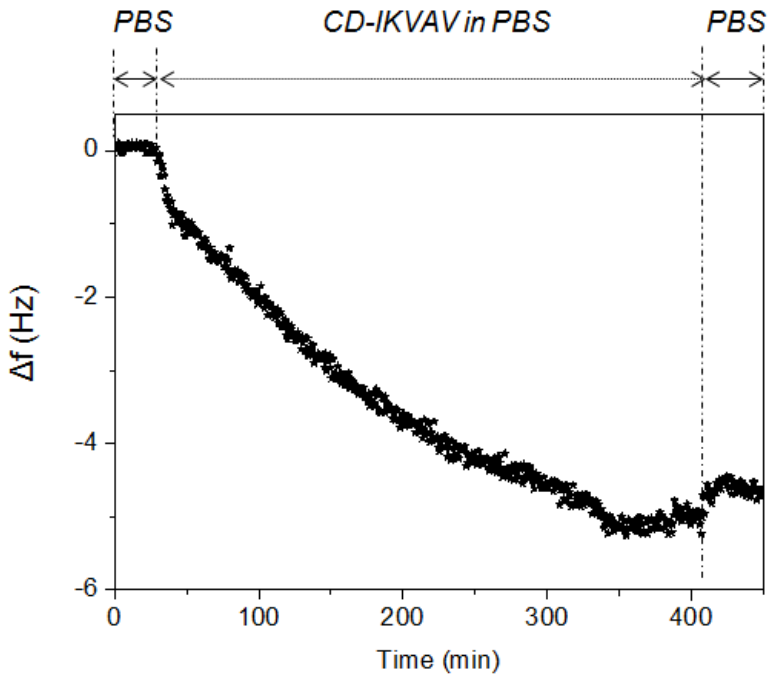


**Figure 6**. QCM-D response curves, in terms of changes in frequency, during the non-covalent conjugation of CD-IKVAV to the self-assembled 100% PS-PEO-Ada surface.

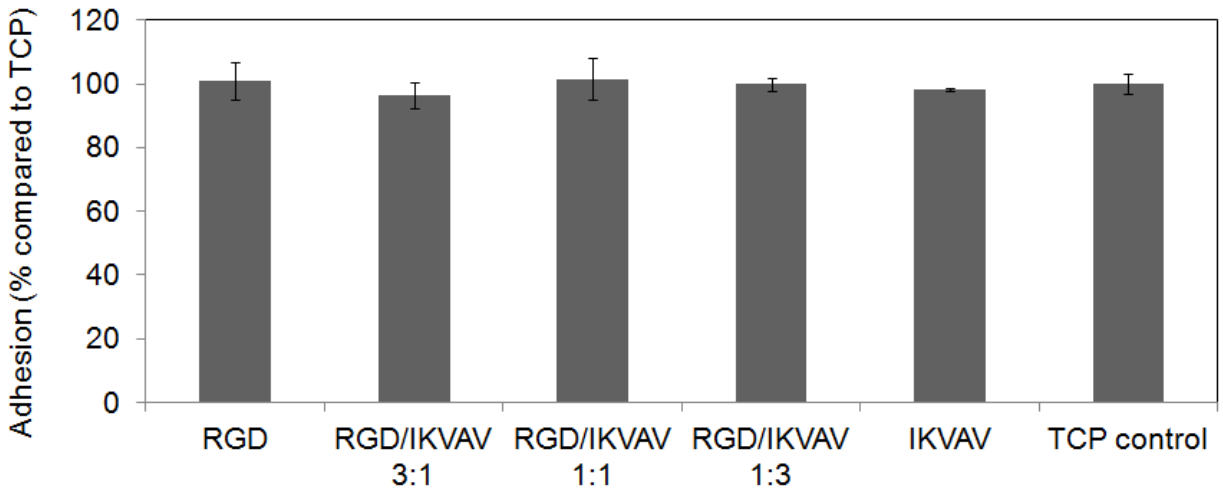


**Figure 7**. Adhesion of hMSCs to self-assembled PS-PEO-Ada surfaces conjugated with different molar ratios of CD-RGD and CD-IKVAV, compared to control TCP. Error bars represent mean ± SD for $n = 4$, $p < 0.05$. All the cells were cultured on the substrates at a density of 3,000 cells/cm$^2$ in serum-free media for a period of 2 hours.

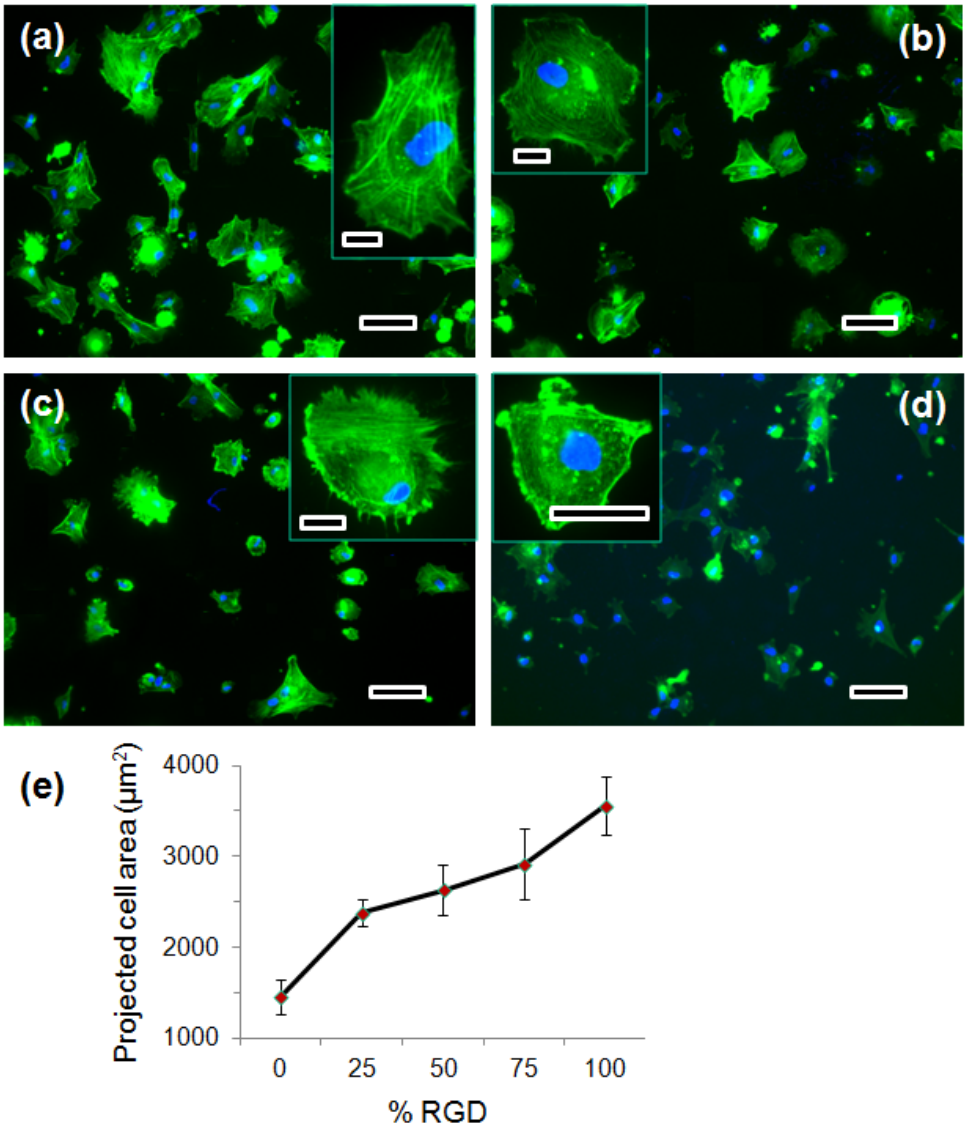


**Figure 8**. Fluorescent microscopy images of hMSCs on self-assembled 100% PS-PEO-Ada surfaces conjugated with different molar ratios of CD-RGD and CD-IKVAV peptide sequences: 75% (a), 50% (b), 25% (c), and 0% (d) of RGD; the projected average cell area as a function of the molar ratio of RGD (e). The scale bars in (a)-(d) are 100 μm (in insets, 20 μm). All the cells were cultured on the substrates at a density of 3,000 cells/cm$^2$ in serum-free media for a period of 24 hours.

SCHEMES.

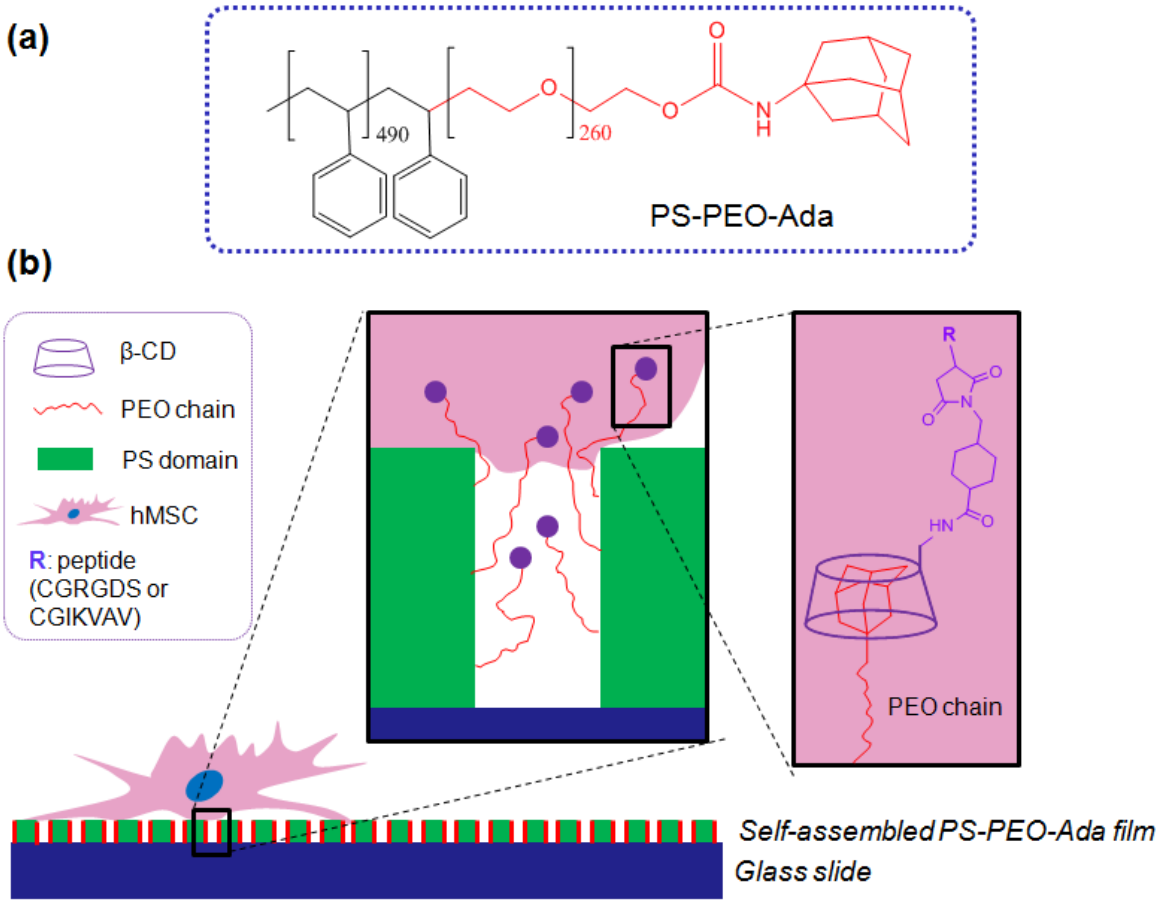


**Scheme 1.** Molecular structure of PS-PEO-Ada (a), schematic illustration of the cross section of the peptide conjugated self-assembled PS-PEO-Ada surfaces (b).

AUTHOR INFORMATION

**Corresponding Author**

*Tel.: +61 3346 3858. E-mail: j.cooperwhite@uq.edu.au.

ACKNOWLEDGMENT

The authors would like to acknowledge the financial support provided by the Australian Research Council Discovery Grant Scheme (DP1095429). This work was performed in part at the Queensland node of the Australian National Fabrication Facility, a company established under the National Collaborative Research Infrastructure Strategy to provide nano and microfabrication facilities for Australian researchers.

REFERENCES

(1) Hudalla, G. A.; Murphy, W. L. *Langmuir* **2010**, *26*, 6449-6456.

(2) Joddar, B.; Ito, Y. *J. Mater. Chem.* **2011**, *21*, 13737-13755.

(3) Bae, J. W.; Lee, E.; Park, K. M.; Park, K. D. *Macromolecules* **2009**, *42*, 3437-3442.

(4) Yoon, J. J.; Song, S. H.; Lee, D. S.; Park, T. G. *Biomaterials* **2004**, *25*, 5613-5620.

(5) Figueiras, A.; Carvalho, R. A.; Ribeiro, L.; Tirres-Labandeira, J. J.; Veiga, F. J. B. *Eur. J. Pharm. Biopharm.* **2007**, *67*, 531-539.

(6) Zhang, G.; Wang, X.; Shi, X.; Sun, T. *Talanta*, **2000**, *51*, 1019-1025.

(7) Willians, R. O.; Mahaguna, V.; Sriwongjanya, M. *Eur. J. Pharm. Biopharm.* **1998**, *46*, 355-360.

(8) Habus, I.; Zhao, Q.; Agrawal, S. *Bioconjugate Chem.* **1995**, *6*, 327-331.

(9) Valle, E. M. M. D. *Proc. Biochem.* **2003**, *39*, 1033-1046.

(10) Loftsson, T.; Duchêne, D. *Int. J. Pharm.* **2007**, *329*, 1-11.

(11) Lin, Z. Q.; Kim, D. H.; Wu, X. D.; Boosahda, L.; Stone, D.; LaRose, L.; Russell, T. P. *Adv. Mater.* **2002**, *14*, 1373-1376.

(12) George, P. A.; Cooper-White, J. J. *Eur. Poly. J.* **2009**, *45*, 1065-1071.

(13) George, P. A.; Doran, M. R.; Croll, T. I.; Munro, T. P.; Cooper-White, J. J. *Biomaterials* **2009**, *30*, 4732-4737.

(14) Stevens, M. M.; George, J. H. *Science* **2005**, *10*,1135-1138.

(15) Dalby, M. J.; Gadegaard, N.; Tare, R.; Andar, A.; Riehle, M. O.; Herzyk, P.; Wilkinson, D. D.; Oreffo, R. O. C. *Nat. Mater.* **2007**, *6*, 997-1003.

(16) Frith, J. E.; Mills, R. J.; Cooper-White, J. J. *J. Cell Sci.* **2012**, *125*, 317-327.

(17) Hirschfeld-Warneken, V. C.; Arnold, M.; Cavalcanti-Adam, A.; López-García, M.; Kessler, H.; Spatz, J. P. *Euro. J. Cell Bio.* **2008**, *87*, 743–750.

(18) Ghaemi, S. R.; Harding F. J.; Delalat, D.; Gronthos, S.; Voelcker, N. H. *Biomaterials* **2013**, *34*, 7601-7615.

(19) Uccelli, A.; Moretta, L.; Pistoia, V. *Nat. Rev.* **2008**, *8*, 726-736.

(20) Tang, W.; Ng, S. C. *Nat. Protoc.* **2008**, *3*, 691-697.

(21) Serro, A. P.; Carapeto, A.; Paiva, G. J.; Farinha, P. S.; Colaco, R.; Saramago, B. *Surf. Interface Anal.* **2012**, *44*, 426-433.

(22) Rangelov, S.; Trzebicka, B.; Janroz-Piegza, M.; Dworak, A. *J. Phys. Chem. B* **2007**, *111*, 11127-11133.

(23) George, P. A.; Donose, B. C.; Cooper-White, J. J. *Biomaterials* **2009**, *30*, 2449-2456.

(24) Hynes, R. O. *Cell* **1992**, *69*,11-25.

(25) Maheshwari, G.; Brown, G.; Lauffenburger, D. A.; Wells, A.; Griffith, L. G. *J. Cell Sci*. **2000,** *113*, 1677-1686.

(26) Rossier, O.; Octeau, V.; Subarita, J.-B.; Leduc, C.; Tessier, B., Nair, D.; Gatterdam, V.; Destaing, O.; Albigès-Rizo, C.; Tampé, R.; Cognet, L.; Choquet, D.; Lounis, B.; Giannone, G. *Nat. Cell Biol.* **2012**, *14*, 1057–1067.

TOC Figure

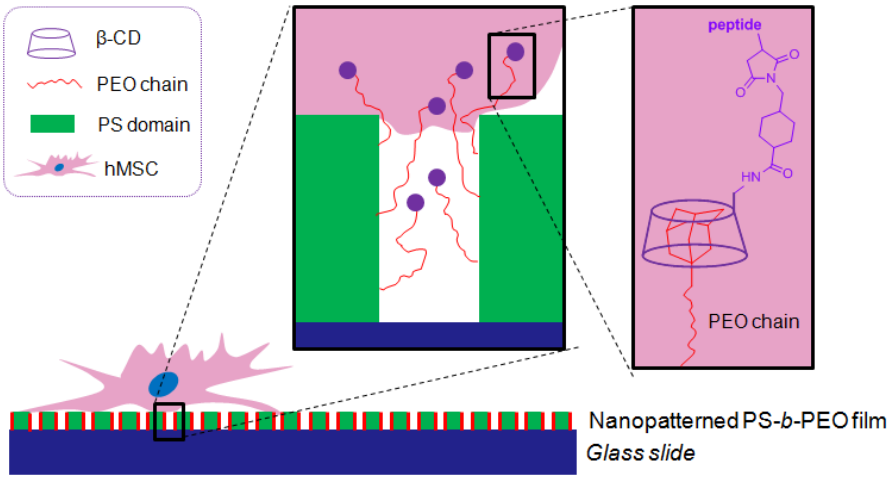
β-CD
PEO chain
PS domain
hMSC
peptide
PEO chain
Nanopatterned PS-*b*-PEO film
*Glass slide*